ELSEVIER

Palaeogeography, Palaeoclimatology, Palaeoecology 199 (2003) 167–185

PALAEO

www.elsevier.com/locate/palaeo

Climate change during Cenozoic inferred from global carbon cycle model including igneous and hydrothermal activities

Hirohiko Kashiwagi *, Naotatsu Shikazono

Department of Applied Chemistry, Faculty of Science and Technology, Keio University, 3-14-1, Hiyoshi, Kouhoku-ku, Yokohama 223-8522, Japan

Received 18 January 2002; accepted 13 June 2003

Abstract

This paper discusses climate change in the Cenozoic by constructing a global carbon cycle model which is based on the GEOCARB-type model. Major improvements over previous models in this study are as follows. Previous models have not considered CO_2 behavior at subduction sufficiently. They do not distinguish at subduction zones between the CO_2 degassing from a back-arc basin (BAB) and that from an island-arc, although their degassing mechanisms may be different and should be treated separately. Also, previous models might overestimate the effect of silicate weathering in the regions of the Himalayan and Tibetan Plateau (HTP) on CO_2 drawdown. Recent studies have revealed that this is smaller than previously presumed. Thus, we deal with these two kinds of degassing independently, and estimate the contribution of silicate weathering based on their studies. They are incorporated into the model. The model results indicate that: (1) the contribution of silicate weathering in the HTP region is small; (2) the warming from late Oligocene to early Miocene might be due to the CO_2 degassing from the BAB; (3) the cooling event in the middle Miocene (15 Ma) is caused by a large amount of the organic carbon burial; (4) the CO_2 variation is well consistent with the other studies of CO_2 estimate, especially with the recent studies of CO_2 estimate from the Miocene which indicate a relatively low level of CO_2; (5) the age discrepancy between the CO_2 peak in our model and the period of the Miocene Climatic Optimum might be attributed to the uncertainty of estimate of the BAB production rate, as a result of which the estimate should be revised. The model does not reconstruct the cooling trends from the middle Miocene (about 15 Ma) and the cooling event at the Eocene/Oligocene (E/O) boundary. This mismatch cannot be explained by the uncertainty of parameter estimates. Concerning the former event, the CO_2 increase of the middle Miocene in our model may be consistent with increased volcanic activity resulting in a large amount of CO_2 degassing. Therefore, it could be indicated that the coolings from 15 Ma and at the E/O boundary are attributed to the change of latitudinal temperature distribution caused by the variations of the oceanic environments, because the current carbon cycle models are not able to consider factors other than the CO_2 greenhouse effect in estimation of surface temperature. However, the change of the temperature distribution on the surface itself does not affect the global averaged temperature. This assumption might not be precise because of the effects of in-depth heat exchange and other climatic factors. Nevertheless, a numerical test of the latitudinal sea surface temperature distribution based on observed $\delta^{18}O$ records indicates that these effects are not critical at least for the coolings at the

* Corresponding author. Tel.: +81-45-563-1141 ext. 42354; Fax: +81-45-566-1551.
E-mail address: h.kashiwagi@mmm-keio.net (H. Kashiwagi).

0031-0182/03/$ – see front matter
doi:10.1016/S0031-0182(03)00506-6

E/O boundary and from 15 Ma. Thus, the result of our model still reflects the reasonable mean temperature at least as a global one, and at the same time, the accurate reconstruction of the above two coolings might be beyond our carbon cycle model.

Keywords: carbon dioxide; paleoclimatology; Cenozoic; back-arc basin; degassing; weathering

1. Introduction

Atmospheric carbon dioxide plays an important role in climate change on the geological time scale ($>10^6$ yr scale), based not only on geological records but also on computational models (Budyko and Ronov, 1979; Berner et al., 1983). Atmospheric CO_2 level on the geological timescale is regulated by the global carbon cycle which involves silicate weathering, carbonate weathering, carbonate precipitation, organic carbon burial, carbonate metamorphism, mantle degassing and so on (e.g. Berner et al., 1983).

Several computational models of long-term carbon cycle have been constructed. For example, Berner (1994) constructed a model for Phanerozoic time, and Lasaga et al. (1985) and Tajika (1998) dealt with the global carbon cycle for the last 100 and 150 million years, respectively. Berner (1994) indicated a high CO_2 level during the Mesozoic and a decrease in CO_2 during the Cenozoic. Tajika (1998) concluded that the warming in the Cretaceous resulted from increased tectonic forcing such as volcanic activities, and that the cooling in the Cenozoic resulted from enhanced erosion rate due to the formation and uplift of the Himalayan and Tibetan Plateau (HTP). Recently, a revised GEOCARB model has been developed by Berner and Kothavala (2001), which introduces some new or modified methods of parameterizations, i.e. an equation of the global mean temperature and CO_2 which is based on new GCM results, consideration of the effects of volcanic weathering, both in subduction zones and on the seafloor, as well as paleo-landarea and paleo-runoff. These previous studies are generally in agreement with the geological record. However, they do not discuss the climate events in the Cenozoic. Besides, there are some climate events which have not been reconstructed in the previous models, i.e. the warming event around 17–16 Ma (e.g. Flower, 1999), and the warming from the late Oligocene to early Miocene (e.g. Kaiho, 1989).

In the cooling trend through the Cenozoic, some climate events are inferred from various kinds of studies (see Section 2). In this paper we first discuss these main climate events in the Cenozoic, and then construct global carbon cycle models in order to consider the causes and effects of the global carbon cycle on the Cenozoic climate changes.

2. Climatic events in the Cenozoic

In this section we discuss some climatic events in the Cenozoic and the problems in a global carbon cycle model which have to be modified. One of the most general methods to infer climate change is the analysis of deep-sea oxygen isotope records (Fig. 1). Although the oxygen isotope data provide constraints on the evolution of not only deep-sea temperature but also continental

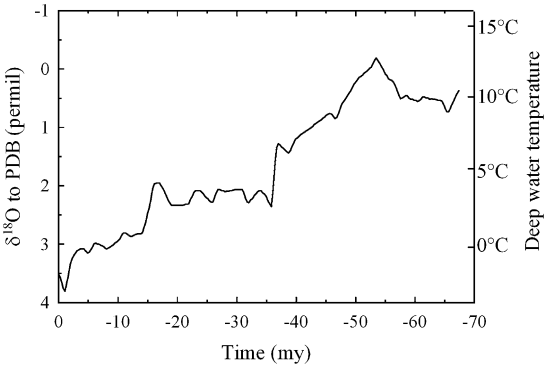

Fig. 1. Deep-water temperature and $\delta^{18}O$ variations during the Cenozoic (after Shackleton, 1987). Temperature estimate (right axis) is based on the model of Shackleton and Kennett (1975).

ice-volume (Zachos et al., 2001), they still play a very important role to estimate climate change.

2.1. Cooling events

Two rapid cooling events during the Cenozoic have been pointed out by many studies. One is likely to have occurred at the Eocene/Oligocene boundary (about 36 Ma), the other in the middle Miocene (about 15 Ma).

Concerning the cooling at the E/O boundary, although the change of the CO_2 level might be partially associated with the climate event because a change of $\delta^{13}C$ is reported (e.g. Shackleton and Hall, 1984), this cooling is generally believed to be related to oceanic environmental change. For example, the Antarctic Circumpolar Current (ACC) was formed in this period, generating cold deep water (e.g. Keller et al., 1987).

The rapid cooling event in the middle Miocene and the subsequent cooling trend to the Present have been pointed out by many studies (e.g. Savin et al., 1975). In this respect, Vincent and Berger (1985) suggested the 'Monterey Hypothesis', i.e. the increased burial of organic carbon would have lowered atmospheric CO_2 and decreased the atmospheric surface temperature. This burial rate may be evaluated by using the global carbon cycle models based on the $\delta^{13}C$ variations in the ocean.

The possibility that deep-water circulation was related to the 15 Ma cooling trend was pointed out by e.g. Woodruff and Savin (1989). They indicated that this period corresponds to the beginning of the formation of North Atlantic Deep Water. It would have been developed strongly from the middle Miocene onwards (Blanc and Suplessy, 1982). The period of this cooling seems to be also coincident with the expansion of the Antarctic ice-sheets (Savin et al., 1975; Shackleton and Kennett, 1975). This expansion is thought to have resulted from the falling temperature in this region. Pagani et al. (1999) and Kump and Arthur (1997) also correlated the expansion of the ice-sheets with the decreased high-latitude temperature.

The suggestion that increased weathering caused more CO_2 consumption and cooling has been debated strongly (e.g. Raymo et al., 1988). This kind of the explanation is based on the fact that the strontium isotope ratio ($^{87}Sr/^{86}Sr$) in the ocean increased in the late Cenozoic. This period also corresponds to the beginning of uplift of the HTP. According to Tajika (1998), the rapid cooling event around 15 Ma may have been the result of increased silicate weathering in the HTP region. He concluded that silicate weathering in the HTP region would have lowered the atmospheric CO_2 level, and that this could explain the increase of $^{87}Sr/^{86}Sr$ in the ocean during the late Cenozoic, which could not be explained by the model of Berner (1994).

However, in the model result of Tajika (1998), the subsequent cooling trend from the middle Miocene may not be consistent with some geological and biological studies. Temperature declined rapidly near 15 Ma, but soon increased to more than the present surface temperature. We may not be able to regard this as a 'subsequent cooling trend' from 15 Ma.

Tajika (1998) introduced a free parameter, β, which represents the contribution of dissolution of Ca from the HTP region and the eroded HTP materials into the ocean to the worldwide total supply of Ca due to chemical weathering. It includes the weathered and dissolved cation not only on the continent but also in the ocean.

However, weathering in the ocean would not be the critical amount (e.g. Berner and Kothavala, 2001), compared to that on the continents. Because riverine Sr flux in the HTP region would account for about 22% of the worldwide flux (Palmer and Edmond, 1989), β, which ranges from 0.25 to 0.45 in his model, would be somewhat large.

Moreover, because the value of 22% includes not only silicate-derived but also carbonate-derived strontium flux, the contribution of the silicate weathering flux from continents might be less than 22%. In this respect, several studies showed that carbonate minerals play a more important role in the weathering of the HTP region than silicate minerals. The mass-balance calculations by Blum et al. (1998) indicated that 82% of the HCO_3^- flux is derived from the weathering of carbonate minerals and that only 18% is derived

from silicate weathering in the Himalayan rivers. This is consistent with the conclusion by Krishnaswami et al. (1992), who indicated that about two-thirds of the dissolved cations are derived from carbonate weathering and about one-third from silicate weathering in the Ganges–Brahmaputra and Indus rivers. These results also correlate with the result by Karim and Veizer (2000) who showed that the discharge weighted mean contribution of silicate derived $Ca^{2+}+Mg^{2+}$ is about one-fourth. Kerrick and Caldeira (1999) also calculated the influence of silicate weathering in the HTP region to be small. The carbonate discussed here was derived from metamorphosed carbonate rocks or soil carbonate, whose strontium isotope ratio is much higher than marine calcite, because it originated from weathered silicate minerals (Quade et al., 1997). High $^{87}Sr/^{86}Sr$ values of these minerals might be explained by the increase of $^{87}Sr/^{86}Sr$ in the ocean (Kashiwagi and Shikazono, 2001). Furthermore, disseminated calcite with very high $^{87}Sr/^{86}Sr$ in the Raikhot watershed and other locations within the Nanga Parbat Massif of northern Pakistan has been identified (Jacobson and Blum, 2000).

Therefore, the observed rapid increase of $^{87}Sr/^{86}Sr$ in seawater (e.g. Burke et al., 1982) from the late Cenozoic could be attributed to carbonate weathering with high $^{87}Sr/^{86}Sr$ rather than silicates. In addition, in the weathering process carbonate weathering has no net effect on the amount of atmospheric CO_2, while 1 mole of atmospheric CO_2 is consumed by 1 mole of Ca or Mg silicate weathering (e.g. Berner, 1994).

Thus, the effect on atmospheric CO_2 presumed by the increase of the strontium isotope record might be much less than the result by Tajika (1998). In this paper, we reevaluate the contribution of silicate weathering in the HTP region by using a global carbon cycle model.

2.2. Warming events

Three remarkable warming events seem to have occurred during the Cenozoic. The warming in the early Eocene is one of them. The cause is often attributed to the greenhouse effect of CO_2 (e.g. Rea et al., 1990). It might have resulted from active volcanism at the mid-ocean ridges. The results of the numerical models of Berner (1994) and Tajika (1998) showed an increased CO_2 level during this period, because the degassing flux of CO_2 increases owing to the large sea-floor spreading rate at that period. Because this climate event could be generally reconstructed by the carbon cycle models available so far, it is not discussed in detail in this paper. We focus on the other two events, i.e. the Miocene Climatic Optimum (MCO) and warming from the late Oligocene to early Miocene.

2.2.1. The Miocene Climatic Optimum

The MCO is believed to have occurred at range from 17 to 14.5 Ma (Flower, 1999). The warmth may have been global, although it may not have been as warm as in the early Eocene. Based on oxygen isotope records, Shackleton and Kennett (1975) pointed out that the temperature of high-latitude surface water may have been almost the same as that during the late Eocene. Savin et al. (1975) also indicated that temperatures of deep water and high-latitude surface water were higher than today by 6°C. As well, the studies of paleovegetation (Yamanoi, 1993), of paleotemperature estimates based on floras (Axelrod and Baily, 1969) and of oxygen isotope composition of marine shells (McGrowan and Li, 1997) suggested this warming event.

This warming event has not been reconstructed in the previous global carbon cycle models. Based on the assumption that the climate changes from the Cretaceous were dominantly influenced by the CO_2 level, as generally believed (e.g. Budyko and Ronov, 1979), the MCO would have resulted from increase of CO_2.

In fact, it is often said that the greenhouse effect of CO_2 contributed to the warming optimum. For example, Camp (1995) suggested that this warming may have been caused as a result of the eruption of huge amount of Columbia River basalt which might have released CO_2 to lead to the 3-K increase by the greenhouse effect (Coffin and Eldholm, 1993). In the Japanese Islands, Ti-rich Icelandite-like and Mg-rich basaltic activities occurred during this period (Dudas et al., 1983). This type of basaltic magma is thought to have

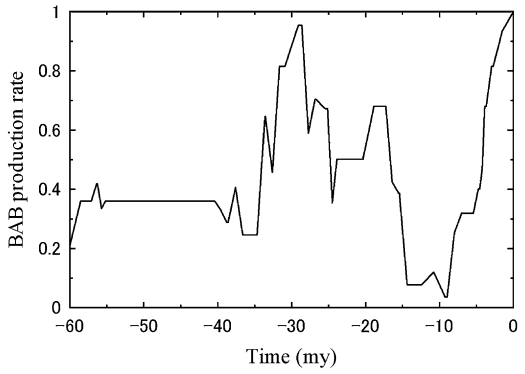

Fig. 2. Variation in relative rates of production of back-arc basins in the Cenozoic estimated by compilation of the crustal production of 29 back-arc basins in the world (after Kaiho and Saito, 1994). This is used as a parameter of the degassing flux from back-arc basins at subduction zones in the model.

been generated at deep mantle which may have been related to mantle plume activity (Tatsumi et al., 1989). Such a mantle plume may have released a large amount of CO_2 to the atmosphere.

Moreover, another approach to estimate CO_2 degassing in this period is pointed out. Shikazono (2003) noted the high concentration of CO_2 in hydrothermal water at back-arc basins (BABs). Shikazono (1998, 1999) suggested that CO_2 degassing from BABs might have an influence on the atmospheric CO_2 levels, thus the climate change on geological time scale. He calculated the hydrothermal CO_2 degassing flux from a BAB (this calculation is modified in this paper, see below), and found that it might have influenced global climate change.

The significance of BABs to climate change was also pointed out by Kaiho and Saito (1994). They selected 29 BABs in the world, and calculated the production rate for each spreading interval by using the area of spreading and its averaged thickness (Fig. 2).

They concluded that climate changes between 30 and 5 Ma may roughly correlate with the variation of crustal production rate of BAB. The result also shows a high peak of crustal production of back-arc basins also in the period of the MCO, which might possibly indicate that the MCO was related to crustal production of a back-arc basin. They considered that sea-level variation due to crustal production might have caused climate change, but the degassing flux of CO_2 should be noted when we pay attention to large flux of CO_2 from back-arc basins.

2.2.2. Warming from the late Oligocene to early Miocene

Gradual warming from the late Oligocene to early Miocene as well as the warming from the late Oligocene to early Miocene, mentioned above, have been pointed out based on $\delta^{18}O$ of foraminiferal carbonate (Miller et al., 1987; Kennett and Barker, 1990). Kaiho (1989) proposed the oxygen index (OI) to estimate global changes in the oxygen content of deep oceanic waters. OI is defined as the ratio of aerobic benthic foraminifera forms vs. aerobic plus anaerobic ones in deep sea. It can be used to extrapolate relative amounts of dissolved oxygen in deep-sea bottom water.

In the warming period, cold seawater in high latitudes would have declined and the velocity of deep-sea circulation would have been lowered. As a result, the supply of oxygen to deep sea would have decreased, combined with a lower dissolution rate of oxygen due to higher temperature, which means low OI. Based on this assumption, he suggested OI as an index to estimate paleoclimate change. He found that periods of low OI in the late Paleocene to early Eocene and late Oligocene to early Miocene seem to be consistent with those suggested to have been warm.

Moreover, Kaiho and Saito (1994) also indicated that the higher rates of crustal production in BAB from the late Oligocene to early Miocene seem to be consistent with the warming during that period.

It can be suggested that these two warming events (the MCO and the warming from late Oligocene to early Miocene times) are commonly related to BAB. In fact, MCO has not been reconstructed by the previous models, which do not consider BAB explicitly. Thus, we discriminate the degassing of CO_2 from between BAB and island-arc as that from subduction zones in the model explicitly.

2.3. CO_2 degassing at subduction zones

In a global carbon cycle model, it is very important to decide parameters governing the rate of CO_2 degassing, because the rate exerts a critical influence on the atmospheric CO_2 level (cf. Berner et al., 1983). Therefore, we discuss the degassing history of the late Miocene and the degassing and regassing parameters to be used in the model.

2.3.1. Increased volcanic activity from the middle Miocene

Several studies indicate intense volcanic activity (hence CO_2 degassing) in the late Miocene at subduction zones. For example, the number of early Oligocene to Recent volcanic ash horizons recorded in the Philippine Basin region is compared with the rate of accumulation of total volcanic debris (Donnelly, 1973; Kennett et al., 1977). Their general trends are in good agreement with each other, and it is indicated that the volcanic activity may have increased during the late Miocene (approximately 10 Ma). Histograms of K–Ar dates with relative volumetric estimates of igneous rocks erupted in the Circum Pacific region by Kennett et al. (1977) and in the Japanese Islands (Tsunakawa, 1981) also support the increasing trend in volcanic activity. Moreover, the production rate of BAB by Kaiho and Saito (1994) might indicate the increasing trend.

These studies also indicate that volcanic activity at a subduction zone seems to have increased in the late Miocene, while the intensity of igneous activity at the mid-ocean ridge would have decreased in the Cenozoic as a general trend. Volcanic activity at a subduction zone might not be synchronized with those at the mid-ocean ridge.

Considering that the CO_2 degassing flux from mid-ocean ridges is larger than that from subduction zones (Sano, 1996), the result of the global carbon cycle model should indicate less decrease or some increase of CO_2 in the late Miocene than the previous models due to the large amount of the degassing flux at subduction zones and increased volcanic activity in the late Miocene, because the previous models have not included degassing parameters which reflect the increased volcanic activity at subduction zones from the late Miocene.

2.3.2. Parameters in relation to degassing fluxes

The degassing flux at a subduction zone may strongly depend on the amount of subducted materials (e.g. carbonate minerals and organic carbon), and thus it could be assumed that the production rate of the oceanic crust (i.e. the seafloor spreading rate) roughly equals to the subduction rate at the subduction zone. It is the reason for the assumption that the degassing flux is proportional to the seafloor spreading rate in the previous carbon cycle models (e.g. Berner et al., 1983), and the treatment of the CO_2 degassing rate both at the mid-ocean ridge and subduction zone as a function of the seafloor spreading rate is quite reasonable as a first approximation.

However, because we take into account the spreading rate of back-arc basins, we should modify the assumption that the seafloor spreading rate corresponds to the subduction rate. It is because crustal production occurs not only at the mid-ocean ridge but also at the back-arc basin in our model. The seafloor spreading rate would not preferably be equal to the subduction rate. Thus, we use the subduction rate, not the seafloor spreading rate, to represent the volcanic activity at the subduction zone.

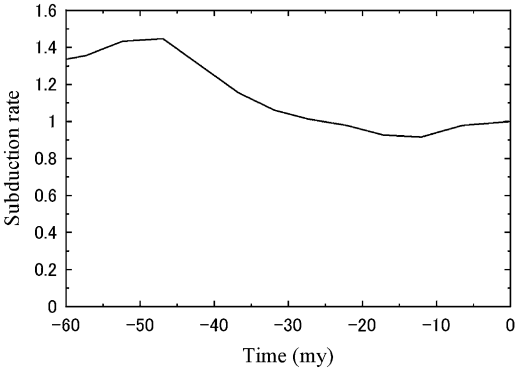

Fig. 3. Subduction rate vs. time estimated by summing the total area of the subducted lithosphere (after Engebreston et al., 1992). This is used as a parameter of the degassing flux from island-arcs at subduction zones in the model.

In our model, while the seafloor spreading rate by Kaiho and Saito (1994) is adopted as a parameter of mid-ocean ridge degassing, the subduction rate calculated by Engebreston et al. (1992) is used as a parameter of subduction zone degassing. This rate is obtained by using subduction zone lengths, not ridge lengths which are generally used to estimate the spreading rate. It also corresponds accurately to the sea-level curve by Haq et al. (1987). Thus, to use subduction length may be preferable in order to consider the activity of the subduction zone. The subduction rate of Engebreston et al. (1992) shown in Fig. 3 is used for the parameter of the CO_2 'regassing' flux, which subducts under the continental crust and is reabsorbed into the mantle (see Tajika, 1998).

Fig. 3 shows a slight increase of the middle Miocene rate, although it is not so clear. Instead, the production rate of BAB by Kaiho and Saito (1994) (Fig. 2) shows an obvious increase, which might indicate the increased volcanic activity at the subduction zone as mentioned above in the model.

3. Model

We construct a global carbon cycle model, which is based mainly on the GEOCARB model developed by Berner (1994) and Berner and Kothavala (2001) and the model by Tajika (1998) which modified the GEOCARB II model. The model used for atmospheric CO_2 is shown in Fig. 4. The formulation of the greenhouse effect of CO_2 by Caldeira and Kasting (1992) is used in order to estimate the global mean surface temperature. Mass balance and isotope mass balance equations are as follows:

$$\mathrm{d}\,M^{\mathrm{C}}/\mathrm{dt} = -F^{\mathrm{C}}_{\mathrm{W}} - F^{\mathrm{C}}_{\mathrm{D,S}} - F^{\mathrm{C}}_{\mathrm{R}} + F_{\mathrm{P}}$$

$$\mathrm{d}\,M^{\mathrm{O}}/\mathrm{dt} = -F^{\mathrm{O}}_{\mathrm{W}} - F^{\mathrm{O}}_{\mathrm{D,S}} - F^{\mathrm{O}}_{\mathrm{R}} + F_{\mathrm{B}}$$

$$\mathrm{d}\,M^{\mathrm{AO}}/\mathrm{dt} = F^{\mathrm{C}}_{\mathrm{W}} + F^{\mathrm{O}}_{\mathrm{W}} + F^{\mathrm{C}}_{\mathrm{D,S}} + F^{\mathrm{O}}_{\mathrm{D,S}} - F_{\mathrm{B}} - F_{\mathrm{P}} + F_{\mathrm{D,H}} + F_{\mathrm{D,M}} = 0$$

$$\mathrm{d}\,\delta^{\mathrm{C}} M^{\mathrm{C}}/\mathrm{dt} = -\delta^{\mathrm{C}}(F^{\mathrm{C}}_{\mathrm{W}} + F^{\mathrm{C}}_{\mathrm{D,S}} + F^{\mathrm{C}}_{\mathrm{R}}) + \delta^{\mathrm{AO}}\, F_{\mathrm{P}}$$

$$\mathrm{d}\,\delta^{\mathrm{O}} M^{\mathrm{O}}/\mathrm{dt} = -\delta^{\mathrm{O}}(F^{\mathrm{O}}_{\mathrm{W}} + F^{\mathrm{O}}_{\mathrm{D,S}} + F^{\mathrm{O}}_{\mathrm{R}}) + (\delta^{\mathrm{AO}} - \Delta)\, F_{\mathrm{B}}$$

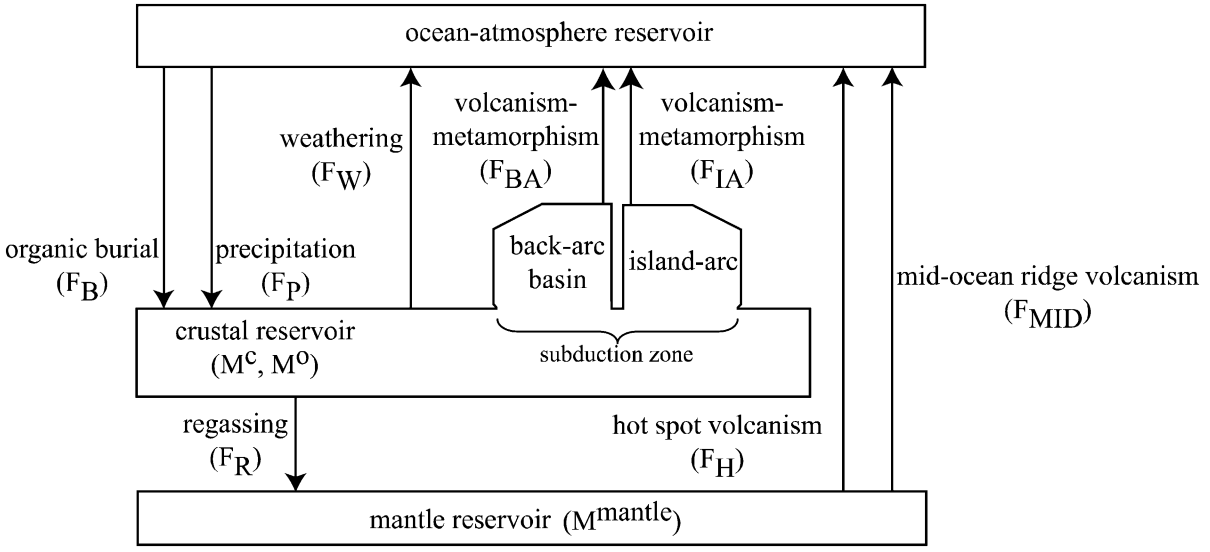

Fig. 4. The carbon cycle model used in this study. Arrows and boxes represent carbon fluxes and reservoirs, respectively. See text for explanation of the symbols. In this model, we distinguish the degassing flux from an island-arc from that from a back-arc basin at the subduction zone (see text).

$$d\,\delta^{AO}M^{AO}/dt = \delta^{C}(F^{C}_{W} + F^{C}_{D,S}) + \delta^{O}(F^{O}_{W} + F^{O}_{D,S}) - (\delta^{AO} - \Delta)F_{B} - \delta^{AO}F_{P} + \delta^{mantle}(F_{D,H} + F_{D,M}) = 0$$

$$d\,M^{ocean}_{Ca}/dt = F^{S}_{W} + F^{C}_{W} - F_{P} = 0$$

where M^{C} is the amount of carbonate carbon in the crustal sediments, M^{O} is the amount of organic carbon in the crustal sediments, M^{AO} is the amount of carbon in the atmosphere–ocean system, F_{W} is the weathering flux, F_{P} is the precipitation flux of carbonate carbon, F_{B} is the burial flux of organic carbon, $F_{D,S}$ is the degassing flux at subduction zones, F_{R} is the regassing flux, $F_{D,H}$ is the degassing flux at hot spot, $F_{D,M}$ is the flux at mid-ocean ridges, δ is the $\delta^{13}C$ value (compiled and modified from Shackleton and Hall, 1984; Shackleton, 1987), and Δ is carbon isotope fractionation factor through the photosynthetic process. Superscripts C, O and S represent carbonate carbon, organic carbon and silicate, respectively. M^{AO} and $\delta^{AO}M^{AO}$ are assumed to be in a steady state (Berner, 1994). All carbonate carbon is regarded as calcite, and calcium is assumed to be transported into the ocean by weathering and precipitated from the ocean. M^{ocean}_{Ca} is also assumed to be in a steady state (Berner, 1994).

Mass fluxes in the above equations are expressed as follows:

$$F^{C}_{W} = k^{C}_{W} f_{BB} f_{LA} f_{AD} M^{C}$$

$$F^{O}_{W} = k^{O}_{W} f_{AD} M^{O}$$

$$F^{S}_{W} = ((1-\beta) f_{B} f^{0.65}_{AD} + \beta f_{R}) F^{S}_{W}{}^{*}$$

$$F_{D,M} = f_{SR} F^{*}_{D,M}$$

$$F_{D,H} = f_{H} F^{*}_{D,H}$$

$$F^{C}_{R} = k^{C}_{R} f_{SUB} f_{C} M^{C}$$

$$F^{O}_{R} = k^{O}_{R} f_{SUB} M^{O}$$

$$f_{BB} = (1 + 0.087\Delta T)\,((2RCO_2)/(1 + RCO_2))^{0.4}$$

$$f_{B} = \exp(0.09\,\Delta T)\,(1 + R\,\Delta T)^{0.65}\,((2RCO_2)/(1 + RCO_2))^{0.4}$$

where ΔT is the temperature difference from the present value, RCO_2 is the ratio of atmospheric CO_2 to the present value, k is the rate constant, f_{BB} is the feedback function for carbonate weathering (Berner, 1994), f_{LA} is the carbonate land area factor (Ronov, 1994; Bluth and Kump, 1991), f_{AD} is the river runoff factor (Ronov, 1994; Otto-Bliesner, 1995), f_{B} is the feedback function for silicate weathering (Berner and Kothavala, 2001), R is the coefficient expressing the effect of temperature on global river runoff (Berner and Kothavala, 2001), f_{SR} is the seafloor spreading rate (Kaiho and Saito, 1994), f_{H} is the production rate of oceanic plateau basalt (Kaiho and Saito, 1994), f_{SUB} is the subduction rate at the subduction zone (Engebreston et al., 1992), f_{C} is the precipitation factor (Berner, 1994), f_{R} is the uplift factor, and β is a parameter which represents the contribution of the Ca dissolution from the HTP region and the eroded HTP materials into the ocean to the worldwide total supply of Ca due to the global chemical weathering today (Tajika, 1998). In this paper, R is 0.045 for colder periods (36–0 Ma) and 0.025 for the rest periods. The value of R is based on Berner and Kothavala (2001), and the value of 36 Ma corresponds to the Eocene–Oligocene boundary.

The CO_2 degassing flux at the subduction zone is expressed as follows:

$$F^{C}_{D,S} = k^{C}_{D,S} f_{SR} f_{C} M^{C}$$

$$F^{O}_{D,S} = k^{O}_{D,S} f_{SR} M^{O}$$

However, as discussed above, the degassing from BAB might play an important role in the climate especially from the late Oligocene to early Miocene and maybe the MCO. Consequently, we divide the CO_2 flux at the subduction zone into the flux at island-arc and that at BAB. Then, degassing fluxes at subduction zones are expressed as follows:

$$F^{C}_{D,S} = F^{C}_{BA} + F^{C}_{IA}$$

$$F^{O}_{D,S} = F^{O}_{BA} + F^{O}_{IA}$$

where F_{BA} is the degassing flux from BAB, and

F_{IA} is the degassing flux at island-arcs. Here we define an index of γ, which represents the contribution of the flux from the back-arc basin to that from the subduction zones at present (that is, $1-\gamma$ is portion of flux from island-arcs).

$$\gamma = (F^{C}_{BA}{}^{*} + F^{O}_{BA}{}^{*})/(F^{C}_{D,S}{}^{*} + F^{O}_{D,S}{}^{*})$$

Because F^{C}_{IA} and F^{C}_{BA}, and F^{O}_{IA} and F^{O}_{BA} are related to M^{C} and M^{O}, respectively, these fluxes are represented as follows:

$$F^{C}_{BA} = k^{C}_{BA}\ M^{C}$$

$$F^{O}_{BA} = k^{O}_{BA}\ M^{O}$$

$$F^{C}_{IA} = k^{C}_{IA}\ M^{C}$$

$$F^{O}_{IA} = k^{O}_{IA}\ M^{O}$$

Rate constants are expressed as follows:

$$k^{C}_{BA} = \gamma f_{BA}\ k^{C}_{D,S}$$

$$k^{O}_{BA} = \gamma f_{BA}\ k^{O}_{D,S}$$

$$k^{C}_{IA} = (1-\gamma) f_{IA}\ k^{C}_{D,S}$$

$$k^{O}_{IA} = (1-\gamma) f_{IA}\ k^{O}_{D,S}$$

where f_{BA} is the production rate of BAB (Kaiho and Saito, 1994), and f_{IA} is a parameter of the degassing flux at subduction zone (Engebreston et al., 1992). See the discussion on parameters in relation to degassing fluxes in Section 2.3).

3.1. Parameter of erosion rate in the HTP region

Berner (1994) introduced an uplift factor, f_R, based on the calculation for the global Sr mass balance. Tajika (1998) considered the global Sr budget as a sum of the HTP and other regions, and used the erosion rate of the HTP region calculated by Richter et al. (1992) to represent the contribution of silicate weathering of this area. However, it may lead to overestimating the influence of silicate weathering to use the strontium isotope ratio to introduce a parameter of silicate weathering in the HTP region. Therefore, another method should be used. Here we adopt a computed elevation history from 45 Ma by Zhao and Morgan (1985) (Fig. 5). Silicate weathering in the HTP region is thought to be related to elevation (e.g. Berner, 1994).

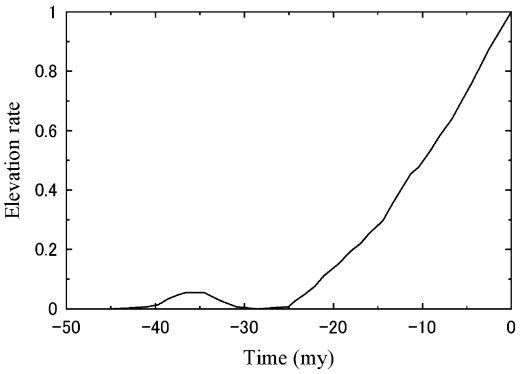

Fig. 5. Elevation rate vs. time estimated by a kinematic model based on plate-tectonic reconstructions and conservation of crustal volume (after Zhao and Morgan, 1985). This is used as a parameter of the elevation in the HTP region (hence weathering flux) in the model.

3.2. Parameter about cation flux in the HTP region at present

As mentioned before, the value of $\beta = 0.25$–0.45 might be overestimated even if β defined by Tajika (1998) includes the flux in the ocean. Instead, we can obtain β, which includes the weathering flux, only on the continents in this model unlike Tajika (1998). The riverine Sr flux in the HTP region is 7.7×10^{15} mol/Ma (Palmer and Edmond, 1989). McCauley and DePaolo (1997) assumed that the riverine Sr flux of silicate weathering accounts for 20% of the modern riverine total Sr flux as the worldwide value, while another study estimates the value to be 40% (Bickle, 1994). Because this value might not be applied in the HTP region, we assumed it to be in the range of 20–40% as a lower estimate. The Sr/Ca and Mg/Ca ratios of average granite are assumed to be 3.5×10^{-3} and 0.5, respectively (Best, 1982). Because Himalayan leucogranites have Sr/Ca ratios not exceeding 10×10^{-3} (Vidal et al., 1982), 3.5×10^{-3} leads to a sufficient upper value for β. Then, the modern flux of silicate in HTP region,

$F^{S}_{W,HTP}$, is calculated to be $0.66–1.32\times10^{18}$ mol/Ma, and β is $F^{S}_{W,HTP}/F^{S}_{W,GLOBAL} = 0.10–0.20$. Here we can assume β to be 0.20 as a large estimate.

3.3. Parameter about flux at BAB at present

We have an estimate of the flux from BAB to consider its significance. Although Shikazono (1999) estimated this flux, the range was too large. Therefore, we try to reevaluate a present flux from BAB.

Shikazono (1999) assumed the CO_2 concentration of hydrothermal solution to be 0.05–0.3 mol/kg. However, we assume it to be 0.03–0.1 because the concentration in most of BAB is within this range (Shikazono, 1999). The crustal production rate is assumed to be 0.94×10^{19} kg/my, and the crustal thickness is set for 2–3 km. While he estimated the seawater/rock ratio to be 5–20, which does not depend on the crustal thickness, we calculated using 2–3 and 5–10 as the seawater/rock ratio because most seawater/rock ratios are within 10 and the seawater/rock ratio decreases with the depth of the crust. The present flux from BAB is estimated to be $0.56–1.88\times10^{18}$ mol/my. The proportion of the flux from BAB to the total subduction degassing (γ) is approximately 0.1–0.3. By using these values, the degassing flux at subduction zones is divided into two fluxes (flux from an island-arc (F_{IA}) and that from BAB (F_{BA})).

The parameters considered in the model are listed in Table 1.

4. Results and discussion

Figs. 6 and 7 show the model results in the cases of the feedback function of Berner and Kothavala (2001) (hereafter referred to as $f_{BB,B}$) and Volk (1987) (hereafter referred to as $f_{BB,V}$), respectively. We compare them to other studies of the CO_2 estimate.

Vertical dashed bars in Figs. 6 and 7 show the paleo-PCO_2 estimate based on the assumption that the fractionation of carbon isotopes during photosynthetic fixation of CO_2 correlates with the concentration of dissolved CO_2 in water (Freeman and Hayes, 1992). In spite of the small number of data, they indicate that the atmospheric CO_2 level generally decreases from the early Cenozoic onwards.

However, on the other hand, some recent studies show that atmospheric CO_2 might have not been changing greatly from the late Cenozoic to the Present.

For example, Cerling (1991) suggested that the CO_2 level in the Eocene may have been lower than 700 ppm (crossed lines in Figs. 6 and 7). Pagani et al. (1999) reconstructed the maximum CO_2 values from ε_P values (the magnitude of car-

Table 1
Explanation and references of parameters for fluxes used in the model

Symbol	Explanation	Reference
f_{LA}	Carbonate land area	Ronov (1994), Bluth and Kump (1991)
f_{AD}	River runoff	Ronov (1994), Otto-Bliesner (1995)
f_B	Feedback function of silicate weathering	Berner and Kothavala (2001)
f_{BB}	Feedback function of carbonate weathering	Berner and Kothavala (2001)
f_R	Uplift factor	Zhao and Morgan (1985)
f_{SR}	Seafloor spreading rate	Kaiho and Saito (1994)
f_H	Production rate of oceanic plateau basalt	Kaiho and Saito (1994)
f_C	Precipitation factor	Berner (1994)
f_{BA}	Production rate of back-arc basin	Kaiho and Saito (1994)
f_{IA}/f_{SUB}	Volcanic activity/subduction rate at subducion zone	Engebreston et al. (1992)
R	Parameter of the effect of temperature on river runoff	Berner and Kothavala (2001); this study (see text)
γ	Contribution of degassing from back-arc basin at subduction zone	See text
β	Contribution of silicate weathering in the HTP region	See text

See text for the details.

bon isotope fractionations during photosynthesis) based on carbon isotopic analyses of diunsaturated alkenones and planktonic foraminifera from the late Oligocene to the late Miocene (bold line in Figs. 6 and 7).

Pearson and Palmer (2000) used the boron-isotope ratios of ancient planktonic foraminiferal shells to estimate the pH of the surface of ocean water (shaded area and vertical bars in Figs. 6 and 7). Their estimates around the Miocene roughly correlate with those by Pagani et al. (1999) except for the slight CO_2 peak in the MCO. Because alkalinity variation is elaborate and poorly constrained by the CCD record to estimate (Pearson and Palmer, 2000), this estimate may have significant errors especially in older age. These errors may have been large at low pH values in the early Cenozoic (Pearson and Palmer, 2000). According to Pearson and Palmer (2000), the CO_2 level in the early Cenozoic is more than

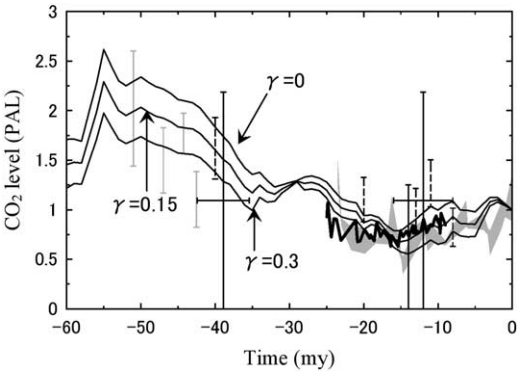

Fig. 6. Atmospheric CO_2 variation for various γ during the last 60 my in the cases for γ=0, γ=0.15, and γ=0.3 in order of height of CO_2, when the feedback function of Berner and Kothavala (2001) is used in the calculation. γ is a parameter which represents the contribution of the flux from a back-arc basin to that from the subduction zones at present. Vertical dashed bars represent the CO_2 estimate of Freeman and Hayes (1992), whose errors are derived from regression statistics and the uncertainty of ±3°C in SST. Crossed lines are the estimates of Cerling (1991), whose errors are based on the uncertainty of estimate of the $\delta^{13}C$ values. Bold line from Oligocene to Miocene is the estimate of Pagani et al. (1999). Shaded area is the estimate of Pearson and Palmer (2000), whose errors are derived from the analytical error of $\delta^{11}B$. We ignore the uncertainties of estimates of age because most of them are small (<1 Ma).

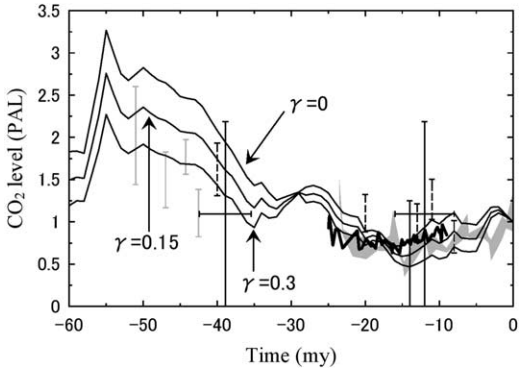

Fig. 7. Atmospheric CO_2 variation for various γ during the last 60 my in the cases for γ=0, γ=0.15, and γ=0.3 in order of height of CO_2, when the feedback function of Volk (1987) is used in the calculation. See caption of Fig. 6 about explanation of γ, vertical dashed bars, crossed lines, bold line, and shaded area in the figure.

10 PAL, although the minimum estimate at that period is approximately 1.5–2 PAL.

In Fig. 8, the model result for the case with $f_{BB,B}$ is compared to the oxygen isotope records of benthic foraminifera by Shackleton (1987).

4.1. Climate change before the Miocene

We first pay attention to the surface temperature and CO_2 patterns before the Miocene, obtained by our model calculations. The model results of the global mean temperature seems to be well consistent with the $\delta^{18}O$ variation from the Paleocene to the early Miocene except for the cooling event at the E/O boundary (Fig. 8). For example, the warming event around 55 Ma, the subsequent cooling trend, and the warming from the late Oligocene to the early Miocene are comparatively in agreement with each other.

Fig. 8 shows that the relatively stable climate during the Oligocene, which is indicated by the oxygen isotope records, is consistent with the pattern of the model results of CO_2 and temperature, and that the temperature peak around the Oligocene in the model results becomes more notable as γ is larger. Although, unfortunately, we cannot accurately determine the value of γ in our model, approximately 0.15–0.3 might be preferable as a value of γ in Figs. 6 and 7. If we do not take into

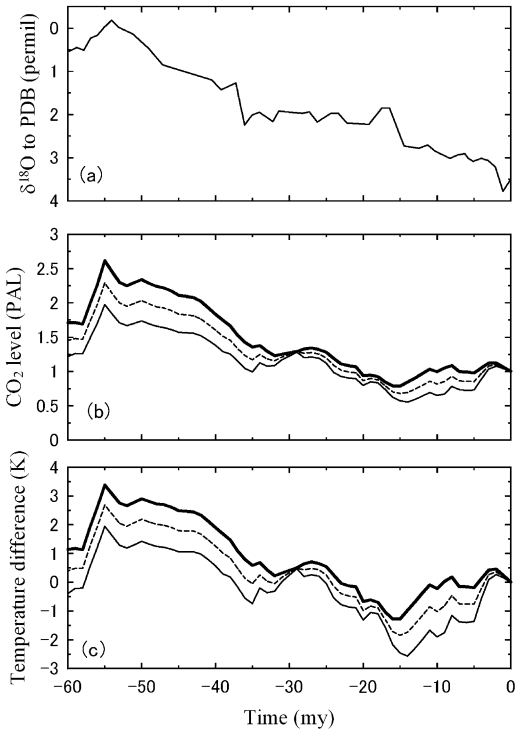

Fig. 8. Comparison of the model results of (b) CO_2 and (c) temperature variations with (a) oxygen isotope records (after Shackleton, 1987) during the last 60 my. Lines in (b) and (c) are the cases for $\gamma=0$, $\gamma=0.15$, and $\gamma=0.3$ in order of height of CO_2. See caption of Fig. 6 about explanation of γ.

account the degassing from BAB ($\gamma=0$), the calculated CO_2 level seems to be somewhat too large. It is indicated that the consideration of BAB activity might explain the Oligocene climate.

On the other hand, in spite of the correlation of the patterns of CO_2 and the temperature variations, the estimated values of CO_2 and temperature of our results seem to be low compared with the $\delta^{18}O$ data, if it is assumed that the warm climate before the late Miocene was caused only by the greenhouse effect of CO_2. Fossil plants indicate that temperature in North America may have been $>10°C$ higher in the Paleocene than at present (Wolfe, 1978). Studies of $\delta^{18}O$ records also suggest an about 10°C warmer climate in the Paleocene than at present (Shackleton and Kennett, 1975; Shackleton, 1984). However, the model results show the low level of CO_2. We will discuss this issue later.

4.2. Climate change from the Miocene

The model results do not indicate a notable high peak of CO_2 at MCO, although the effect of degassing at MCO is pointed out by Camp (1995) and others and the BAB production rate estimated by Kaiho and Saito (1994) has a peak around MCO. However, there is a small peak of CO_2 just before the MCO period (around 19–18 Ma).

Because the difference between the two periods is small, it is possibly derived from the error in estimating the age of the BAB production by Kaiho and Saito (1994). Because they assumed a constant spreading rate of each BAB during its whole spreading interval, their estimates would result in uncertainty of the BAB production rate when some BABs would not have had constant spreading rates. The period of MCO might correspond to that of spreading of the BAB of the Japan Sea. As shown in Kaiho and Saito (1994), the spreading interval of the Japan Sea ranges from the middle Oligocene to the middle Miocene, which includes the period of MCO. If the spreading rate of the Japan Sea is large in the period of MCO, which was suggested based on paleomagnetic data on Miocene rocks in Southwest Japan (Otofuji and Matsuda, 1983, 1987), a higher peak would appear from the calculated production rate of BAB at MCO. Consequently, the model result might show a high peak of CO_2 in the period of MCO.

A low level of CO_2 is found around 15 Ma in our results (Fig. 8). This low CO_2 level in this period is derived from HTP weathering according to the model of Tajika (1998). However, in our results, it is attributed to the shift to the high $\delta^{13}C$ values, and the effect of HTP weathering is rather small. Fig. 9 shows the result of the CO_2 variations for the case where the erosion rate of HTP varies (Zhao and Morgan, 1985) and for the case where the erosion is not considered ($f_R=0$). Apparently, there is little difference between these two results. This is consistent with the conclusions of Quade et al. (1997) and Blum et al. (1998): silicate weathering in the HTP region was not significant for CO_2 drawdown and cooling.

Thus, the relatively low level of CO_2 around

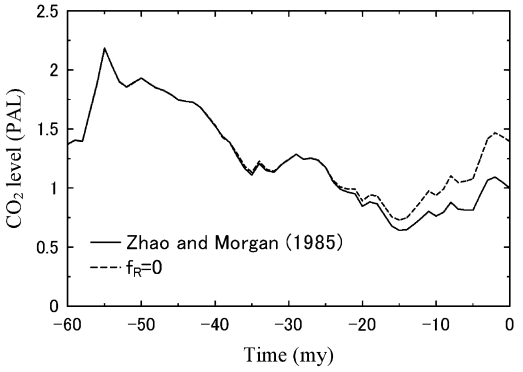

Fig. 9. Atmospheric CO_2 variations for the last 60 my in case of $f_R = 0$ (ignore the HTP uplift) and using the uplift parameter of Zhao and Morgan (1985) (consider the HTP uplift; see Fig. 5). Feedback function of Berner and Kothavala (2001) is adopted in the calculation.

15 Ma is because $\delta^{13}C$ of seawater is high at that time, which reflects large organic carbon burial. This correlates with the Monterey Hypothesis; the cooling at 15 Ma is caused by large amounts of organic carbon burial (Vincent and Berger, 1985).

Our model results of CO_2 from the middle Miocene are supported by other studies. When we use $f_{BB,B}$ (Fig. 6), the CO_2 variation is roughly consistent with the results of Pagani et al. (1999) and Pearson and Palmer (2000). According to the result of our model and the other two isotopic studies, CO_2 level since the Miocene may have been relatively constant but a little bit lower compared to that at present. The CO_2 level slightly increases from the Miocene. When we use $f_{BB,V}$ (Fig. 7), the CO_2 level seems to be lower than that in the case with $f_{BB,B}$, but there is no large difference. The variation pattern of CO_2 is not influenced by the difference between the two feedback functions.

4.3. Disagreement between the model result and oxygen isotope records

Temperature variation since the middle Miocene obtained by our results seems in several respects to be inconsistent with the $\delta^{18}O$ records (Fig. 8). Although various studies including $\delta^{18}O$ records suggest a cooling trend from the middle Miocene onwards (e.g. Shackleton, 1987) (but note that they are partly affected by the ice-volume as mentioned before), our model shows increase of temperature from the middle Miocene, if it is assumed that temperature is governed only by atmospheric CO_2 concentration. We consider the cause of the discrepancy below. First, the error of parameters used in the model is considered.

4.3.1. Uncertainty of parameters in the model

In the model of Tajika (1998), the CO_2 level before 40 Ma is determined by β, which was assumed to be 0.25–0.45 so that the CO_2 level was thought to be consistent with geochemical and other studies. However, because β is estimated to be small in this study, two possible explanations to solve the problem of low levels of CO_2 in our model might be considered as the estimate error of parameters in our model. They are: (1) some factors which 'lower' CO_2 level are overestimated, and/or (2) some factors to 'raise' CO_2 level before the early Cenozoic are missed.

First, we discuss (1). Silicate weathering and organic carbon burial in the carbon cycle would be factors which lower CO_2.

If silicate weathering is the cause of the low CO_2 levels, there would be an error in the calculation of the weathering flux. Because β is small, the difference between the weathering flux before and after the Oligocene is not critical ($0.2F_W^S = 1.3\times10^{18}$ mol/Ma), and the factor of weathering is not important. Thus, the uncertainty in the calculation of the weathering flux might be unlikely.

If estimation of organic carbon burial is the problem, the estimate of the $\delta^{13}C$ value would include an error because the burial flux is basically regulated by $\delta^{13}C$ in our model. However, the isotope value used in our model seems to be reliable as the global records. The spatial variation in the $\delta^{13}C$ content of normal marine sediment carbonate is quite small. The data by Shackleton and Hall (1984) are remarkably similar to those by Shackleton et al. (1985) (Shackleton, 1987). Therefore, organic carbon burial is not thought to be a critical cause of the low CO_2 level.

An important example of (2) might be degassing of CO_2. Degassing fluxes are regarded to be

proportional to their parameter values in our calculations. However, although the assumption would be basically appropriate, it would be very difficult to know how accurate or valid the assumption is.

Furthermore, in our model estimation of f_{BA} is not easy. The low CO_2 level in our model is partially due to a high estimate of the BAB spreading rate (and then large degassing of CO_2) from the middle Miocene by Kaiho and Saito (1994). This high estimate also affects the CO_2 level before the Miocene.

While the production rate drastically increases from 10 Ma, it might be extremely low from 15 to 10 Ma compared to other periods (see Fig. 2). This large gap is one of the causes of the low-level CO_2.

If there is an error in estimating the production rate of BAB from 15 Ma because of the reason mentioned above (for example, some of the BABs which have spread from the Miocene to the Present might have been gradually reducing their spreading rate toward the Present as assumed by Kaiho and Saito (1994), not spreading constantly), the very low production rate from 15 to 10 Ma and drastically increased production rate from 10 Ma might be suppressed. However, it seems not to be probable that the real BAB production rate decreased from 15 Ma, because the increasing production rate of BAB in Kaiho and Saito (1994) from 10 Ma is very large. Moreover, the increase of CO_2 from the late Miocene might be consistent with the increased volcanic activity at subduction zones as mentioned before. Consequently, the CO_2 level in the model would be raised on the whole.

Therefore, the revision of uncertainty of parameter values might be insufficient to decrease CO_2 and then temperature after the middle Miocene, and the decrease of CO_2 from the late Miocene might even not be the case. If it were the case, it could be interpreted that our model results regarding temperature as well as CO_2 level are reasonable, as is discussed below.

4.3.2. Change of latitudinal temperature distribution on the earth

We note that the rapid cooling event at the E/O boundary and the cooling trend from 15 Ma, which are often pointed out by oxygen isotope records, are not reconstructed in our model. These cooling events might be commonly related to the ocean environmental change, especially latitudinal imbalance.

At the E/O boundary, the formation of the ACC prevented heat transport (Keller et al., 1987), resulting in the thermal isolation of Antarctica (Savin et al., 1975) and the change of the latitudinal distribution of temperature as well as the temperature gradient would have been larger (Shackleton and Kennett, 1975). As a result, higher-latitude areas would have been cooled at the E/O boundary. In fact, $\delta^{18}O$ of low-latitude planktonic foraminifera (Shackleton, 1984; Miller et al., 1991) seems to show less increase at the E/O boundary than that of high-latitude planktonic foraminifera (Shackleton and Kennett, 1975), although it should be considered, as mentioned above, that ice formation also raises the value of the $\delta^{18}O$ records. It could be also supported by the observation of Zachos et al. (1993).

The cooling trend from 15 Ma might have been also related to the oceanographic change, the change of the oceanic environment in higher latitudes as well as the cooling event at the E/O boundary. Kennett (1977) indicated the increased temperature gradient between polar and tropical regions during this period. The increase of sea surface temperature in low latitudes as well as the cooling in high latitudes are pointed out (e.g. Savin et al., 1985; Flower and Kennett, 1993).

Finally, both cooling events might be associated with the change of latitudinal temperature distribution and the decreased temperature mainly in higher latitudes. On the other hand, in our model, including other models (GEOCARB models), an equation connecting the CO_2 level with temperature is used (e.g. Caldeira and Kasting, 1992). However, it takes into account the greenhouse effect alone. Other factors, for instance, tectonics and ocean circulation, are assumed to be constant or ignored. Due to this limitation of the present carbon cycle models, it seems to be reasonable that the two cooling events are not reconstructed in our model, also because the equation essen-

tially considers not the latitudinal temperature distribution but the global mean temperature.

As already mentioned, in the periods of these coolings, higher-latitude temperature is estimated to have decreased, while lower-latitude temperature is considered to have not decreased or indeed to have increased. Thus, this observation might mean that these coolings can be ultimately explained by variation of the energy balance or distribution on the surface. If this is true, this variation itself does not influence global mean temperature, even though the change is caused by oceanographic factors. It applies to the case for our carbon cycle model which does not consider the factors other than the greenhouse effect. Thus, we can interpret that, even if the equation to estimate global mean temperature in the carbon cycle models does not take into account factors other than CO_2, they still represent the appropriate temperature at least as a 'global' mean temperature.

However, even local variations of temperature and oceanographic events might cause change of the global environment. The above assumption disregards that tectonics, albedo, atmospheric CO_2 and temperature must be influenced by among them, and that in-depth exchange of the energy (e.g. between the surface and deep sea which potentially contains a large amount of heat capacity) is also probable. Latitudinal imbalance of temperature possibly results in these effects and the errors in the above assumption of energy balance. Accordingly, we examine the possible extent of these effects by a numerical test which uses the $\delta^{18}O$ record which could be a proxy for sea temperature. Unlike the carbon cycle models, it is possible to assume that the $\delta^{18}O$ data record the resultant temperature which includes not only the greenhouse effect but also other factors if we assume that $\delta^{18}O$ represents the temperature variation (but we note that, in fact, $\delta^{18}O$ is also affected by ice-volume). If the calculated mean temperature estimated by the $\delta^{18}O$ record shows the large variation from the middle Miocene (15 Ma) and at the E/O boundary, it can be indicated that the global mean temperature is influenced by the change of the oceanic environment (that is, the factors which are not considered by the global carbon cycle models). Otherwise, it is suggested that the global mean temperature could be regarded to be independent of the ocean environmental change.

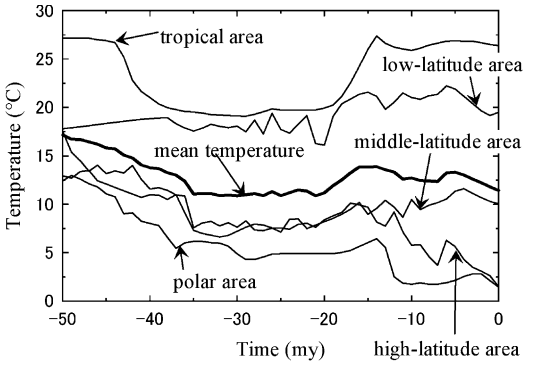

Fig. 10. Variations of the sea surface temperatures in tropical areas (0–10°; Savin et al., 1975), low-latitude (10–20°; Miller et al., 1991), middle-latitude (20–40°; Shackleton, 1986) and high-latitude (40–60°; Shackleton and Kennett, 1975) areas, and the polar region (60–90°; Savin et al., 1975; Shackleton, 1984), as well as the sea surface mean temperature which is calculated by the heat balance of the five areas of temperature.

The numerical examination here assumes that the sea surface temperatures estimated by the $\delta^{18}O$ records reflect the atmospheric temperature. We divide the Earth's surface into five latitudinal areas: tropical area (0–10°), low-latitude area (10–20°), middle-latitude area (20–40°), high-latitude area (40–60°), and polar area (60–90°).

The variations of temperature of the tropical area (T_t), low-latitude (T_l), middle-latitude (T_m), high-latitude (T_h) and polar region (T_p) are based on the oxygen isotope data of planktonic foraminifera of Savin et al. (1975), Miller et al. (1991), Shackleton et al. (1986), Shackleton and Kennett (1975), and Savin et al. (1975), and Shackleton (1984), respectively. When we consider the heat balance on the surface of the earth, the global averaged sea surface temperature (hence surface atmospheric temperature) would be given in this model as follows:

$$T_{mean} = (S_t\ T_t + S_l\ T_l + S_m\ T_m + S_h\ T_h + S_p\ T_p)/$$

$$(S_t + S_l + S_m + S_h + S_p)$$

where S_i is surface area.

Fig. 10 shows the result of each sea surface temperature estimate. In Fig. 10, we find that temperatures in higher-latitude areas generally decline more remarkably around the E/O boundary and from the middle Miocene, while, on the other hand, that in lower-latitude areas do not. The calculated T_{mean} does not show the large fluctuation from 15 Ma and at the E/O boundary. The range of the mean temperature variations since the E/O boundary is also not more than approximately 3°C. Moreover, if it is considered that the $\delta^{18}O$ variations also reflect ice-volume, the 'real' range should be estimated to be less.

Consequently, this calculation could indicate that factors other than the CO_2 greenhouse effect are not effective on the change of the global averaged temperature in the case of variations of the latitudinal energy (or temperature) distribution from 15 Ma and at the E/O boundary. This result leads to the conclusion that the global mean temperature estimated by the global carbon cycle models is appropriate, although the two coolings from 15 Ma and at the E/O boundary do not appear in the model. Preferably, the accurate reconstruction of the two coolings might be outside the framework of our carbon cycle model.

5. Summary and conclusion

We have constructed a modified GEOCARB global carbon cycle model during the Cenozoic, and discussed the relation between the atmospheric CO_2 level and climate change. The important improvements of the model in this study over the previous models are about: (1) the treatment of the CO_2 flux at the subduction zone, and (2) the weathering flux in the HTP regions. With respect to (1), previous models have not distinguished the CO_2 degassing from BAB with that from island-arc at the subduction zone, while their degassing mechanisms might be different from each other. Thus, we deal with these two kinds of degassing independently. The flux of subducted carbon into the mantle should be associated with the subduction rate, while previous models often assume the seafloor spreading rate. Accordingly, we assume that the subducted flux into the mantle is proportional to the subduction rate in the model. With respect to (2), recent studies have indicated that the effect of silicate weathering in the HTP regions on the decrease of atmospheric CO_2 is smaller than previously considered. The calculated result of the contribution of silicate weathering in the HTP region in this study is incorporated into the model.

According to the model results, the consideration of degassing at BAB may explain the warming from the late Oligocene to early Miocene. Moreover, a small peak of CO_2 level is found at 19–18 Ma near the period of the MCO. This discrepancy between the two periods might be due to the estimate error in Kaiho and Saito (1994) which is caused by the assumption of a constant spreading rate of BAB in their active period.

The effect of silicate weathering in the HTP region on the cooling trend since 40 Ma is not significant. The cooling event at 15 Ma relates to increased organic carbon burial (probably the Monterey Hypothesis) rather than to weathering in the HTP region.

The results of the carbon cycle model are compared with those of several studies of CO_2 estimates and oxygen isotope records.

Since the Oligocene, especially the Miocene, the CO_2 variations obtained by our model well correlate with the results of the recent CO_2 estimates by carbon and boron isotope studies (Pagani et al., 1999; Pearson and Palmer, 2000).

However, it is noteworthy that the temperature slightly increases from the middle Miocene towards the Present in our model result. It seems to be inconsistent with the results of oxygen isotope records and other previous studies. Although this might be partially due to the uncertainty of estimate of BAB production rate as mentioned above, it is unlikely that this error completely explains the discrepancy. The CO_2 increase from the early Miocene in our model results might even correlate with increased volcanic activity at the subduction zone from the late Miocene, because CO_2 degassing from the subduction zone accounts for the large amount of total CO_2 degassing.

The cooling at the E/O boundary and the cooling trends from the middle Miocene do not seem to be reconstructed in our model. If these climate

events are commonly associated with the change of temperature distribution over the world due to the ocean environmental change, global mean temperature might not be influenced under the constant total energy on the surface. This assumption is not accurate due to the complicated relationships among tectonics, albedo, CO_2 and temperature and even to these local variations, but the calculation of the global mean temperature by latitudinal temperatures based on the $\delta^{18}O$ records indicates that these effects are not significant for the global mean temperature from 15 Ma and at the E/O boundary. This means that global temperature in our model still represents the probable variation, although it does not take into account factors other than the greenhouse effect in estimating the global mean temperature. Simultaneously, reconstruction of the coolings from 15 Ma and at the E/O boundary may be beyond our carbon cycle models.

Acknowledgements

We are grateful to E. Tajika for checking the manuscript and critical and useful comments. We also thank P.N. Pearson for offering to us the CO_2 data and useful comments. The critical and helpful reviews of R.A. Berner and L.R. Kump are acknowledged.

References

Axelrod, D.I., Baily, H.P., 1969. Paleotemperature analysis of Tertiary floras. Palaeogeogr. Palaeoclimatol. Palaeoecol. 6, 163–195.

Berner, R.A., 1994. GEOCARB II: A revised model of atmospheric CO_2 over Phanerozoic time. Am. J. Sci. 294, 56–91.

Berner, R.A., Kothavala, Z., 2001. GEOCARB III: A revised model of atmospheric CO_2 over Phanerozoic time. Am. J. Sci. 301, 182–204.

Berner, R.A., Lasaga, A.C., Garrels, R.M., 1983. The carbonate–silicate geochemical cycle and its effect on atmospheric carbon dioxide over the past 100 million years. Am. J. Sci. 283, 641–683.

Best, M.G., 1982. Igneous and Metamorphic Petrology. Freeman, New York, 630 pp.

Bickle, M., 1994. The role of metamorphic decarbonation reactions in returning strontium to the silicate sediment mass. Nature 367, 699–704.

Blanc, P.-L., Suplessy, J.-C., 1982. The deep-water circulaiton during the Neogene and the impact of the Messinian salinity crisis. Deep Sea Res. A 29, 1391–1414.

Blum, J.D., Gazis, C.A., Jacobson, A., Chamberlain, C.P., 1998. Carbonate versus silicate weathering on the Raikhot watershed within the High Himalayan Crystaline Seris. Geology 26, 411–414.

Bluth, G.J.S., Kump, L.R., 1991. Phanerozoic paleogeology. Am. J. Sci. 291, 284–308.

Budyko, M.I., Ronov, A.B., 1979. Chemical evolution of the atmosphere in the Phanerozoic. Geochem. Int. 16, 1–9.

Burke, W.H., Denison, R.E., Hetherington, E.A., Koepnick, R.B., Nelson, H.F., Otto, J.B., 1982. Variation of seawater $^{87}Sr/^{86}Sr$ throughout Phanerozoic time. Geology 10, 516–519.

Caldeira, K., Kasting, J.F., 1992. The life span of the biosphere revisited. Nature 360, 721–723.

Camp, V.E., 1995. Mid-Miocene propagation of the Yellowstone mantle plume head beneath the Columbia River basalt source region. Geology 23, 435–438.

Cerling, T.E., 1991. Carbon dioxide in the atmosphere: Evidence from Cenozoic and Mesozoic paleosols. Am. J. Sci. 291, 377–400.

Coffin, M.F., Eldholm O., 1993. Large igneous provinces. Scientific American, October, 42–49.

Donnelly, T.W., 1973. Circum-Caribbean explosive volcanic activity evidence from Leg 15 sediments. In: Edgar, N.T., Saunders, J.B., et al. (Eds.), Initial Reports of the Deep-Sea Drilling Project 15, pp. 969–987.

Dudas, F.O., Campbell, I.H., Gordon, M.P., 1983. Geochemistry of igneous rocks in the Hokuroku district, northern Japan. Econ. Geol. Mon. 5, 115–133.

Engebreston, D.C., Kelley, K.P., Cashman, H.J., Richards, M.A., 1992. 180 million years of subduction. GSA Today, 2, 93–95, 100.

Flower, B.P., Kennett, J.P., 1993. Middle Miocene ocean–climate transition: High-resolution oxygen and carbon isotopic records from deep sea drilling project site 588A, southwest Pacific. Paleoceanography 8, 811–843.

Flower, P., 1999. Warming without high CO_2? Nature 399, 313–314.

Freeman, K.H., Hayes, J.M., 1992. Fractionation of carbon isotopes by phytoplankton and estimates of ancient CO_2 levels. Glob. Biogeochem. Cycles 6, 185–198.

Haq, B.U., Hardenbol, J., Vail, P.R., 1987. The chronology of fluctuating sea level since the Triassic. Science 235, 1156–1167.

Jacobson, A.D., Blum, J.D., 2000. Ca/Sr and $^{87}Sr/^{86}Sr$ geochemistry of disseminated calcite in Himalayan silicate rocks from Nanga Parbat: Influence on river-water chemistry. Geology 28, 463–466.

Kaiho, K., Saito, S., 1994. Oceanic crust production and climate during the last 100 myr. Terra Nova 6, 376–384.

Kaiho, K., 1989. Morphotype changes of deep-sea benthic fo-

raminifera during the Cenozoic Era and their paleoenvironmental implications. Fossils 47, 1–23.

Karim, A., Veizer, J., 2000. Weathering processes in the Indus River Basin: Implications from riverine carbon, sulfur, oxygen, and strontium isotopes. Chem. Geol. 170, 153–177.

Kashiwagi, H., Shikazono, N., 2001. Global strontium cycle and its influence in late Cenozoic. 48th Annual Meeting of the Geochemical Society of Japan, p. 24.

Keller, G., Herbert, T., Dorsey, R., D'Hondt, S., Johnsson, M., Chi, W.R., 1987. Global distribution of late Paleogene hiatuses. Geology 15, 199–203.

Kennett, J.P., Barker, P.E., 1990. Latest Cretaceous to Cenozoic climate and oceanographic developments in the Weddell Sea, Antarctica: An ocean-drilling perspective. In: Barker, P.E., Kennett, J.P. (Eds.), Initial Reports of the DSDP 113B. U.S. Government Printing Office, Washington, DC, pp. 937–960.

Kennett, J.P., 1977. Cenozoic evolution of Antarctic glaciation, the circumantarctic ocean and their impact on global paleoceanography. J. Geophys. Res. 82, 3843–3860.

Kennett, J.P., McBirney, A.R., Thunell, R.C., 1977. Episodes of Cenozoic volcanism in the Circum-Pacific Region. J. Volcanol. Geotherm. Res. 2, 145–163.

Kerrick, D.M., Caldeira, K., 1999. Was the Himalayan orogen a climatically significant coupled source and sink for atmospheric CO_2 during the Cenozoic? Earth Planet. Sci. Lett. 173, 195–203.

Krishnaswami, S., Trivedi, J.R., Sarin, M.M., Ramesh, R., Sharma, K.J., 1992. Strontium isotopes and rubidium in the Ganga–Brahmaputra river system: Weathering in the Himalaya, fluxes to the Bay of Bengal and contributions to the evolution of oceanic $^{87}Sr/^{86}Sr$. Earth Planet. Sci. Lett. 109, 243–253.

Kump, L.R., Arthur, M.A., 1997. Global chemical erosion during the Cenozoic: Weatherability balances the budges. In: Ruddiman, W.F. (Ed.), Tectonic Uplift and Climate Change. Plenum, New York, pp. 399–426.

Lasaga, A.C., Berner, R.A., Garrels, R.M., 1985. An improved geochemical model of atmospheric CO_2 fluctuations over the past 100 million years. In: Sundquist, E.T., Broecker, W.S. (Eds.), The Carbon Cycle and Atmospheric CO_2: Natural Variations Archean to Present. American Geophysical Union, Washington, DC, pp. 397–411.

McCauley, S.E., DePaolo, D.J., 1997. The marine $^{87}Sr/^{86}Sr$ and $\delta^{18}O$ records, Himalayan alkalinity fluxes, and Cenozoic climate models. In: Ruddiman, W.F. (Ed.), Tectonic Uplift and Climate Change. Plenum, New York, pp. 427–467.

McGrowan, B., Li, Q.-Y., 1997. Miocene climatic oscilliation recorded in the Lakes Entrance oil shaft, southern Australia. Aust. J. Earth Sci. 43, 129–148.

Miller, K.G., Fairbanks, R.G., Mountain, G.S., 1987. Tertiary oxygen isotope synthesis, sea level history, and continental margin erosion. Paleoceanography 2, 1–19.

Miller, K.G., Wright, J.D., Fairbanks, R.G., 1991. Unlocking the ice house: Oligocene–Miocene oxygen isotopes, eustasy, and margin erosion. J. Geophys. Res. 96, 6829–6848.

Otofuji, Y., Matsuda, T., 1983. Paleomagnetic evidence for the clockwise rotation of Southwest Japan. Earth Planet. Sci. Lett. 62, 349–359.

Otofuji, Y., Matsuda, T., 1987. Amount of clockwise rotation of Southwest Japan – fan shape opening of the Southwestern part of the Japan Sea. Earth Planet. Sci. Lett. 85, 289–301.

Otto-Bliesner, B.L., 1995. Continental drift, runoff and weathering feedbacks: Implications from climate model experiments. J. Geophys. Res. 100, 11537–11548.

Pagani, M., Arthur, M.A., Freeman, K.J., 1999. Miocene evolution of atmospheric carbon dioxide. Paleoceanography 14, 273–292.

Palmer, M.R., Edmond, J.M., 1989. The strontium isotope budget of the modern ocean. Earth Planet. Sci. Lett. 92, 11–26.

Pearson, P.N., Palmer, M.R., 2000. Atmospheric carbon dioxide concentrations over the past 60 million years. Nature 406, 695–699.

Quade, J., Roe, L., DeCelles, P.G., Ojha, T.P., 1997. The late Neogene $^{87}Sr/^{86}Sr$ record of lowland Himalayan rivers. Science 276, 1828–1831.

Raymo, M.E., Ruddiman, W.F., Froelich, P.N., 1988. Influence of late Cenozoic mountain building on ocean geochemical cycles. Geology 16, 649–653.

Rea, D.K., Zachos, J.C., Owen, R.M., Gingerrich, P.D., 1990. Global change at the Paleogene–Eocene boundary: Climatic and evolutionary consequence of tectonic events. Paleogeogr. Paleoclimatol. Paleoecol. 79, 117–128.

Richter, F.M., Rowley, D.B., DePaolo, D.J., 1992. Sr isotope evolution of seawater: The role of tectonics. Earth Planet. Sci. Lett. 109, 11–23.

Ronov, A.B., 1994. Phanerozoic transgressions and regressions on the continents: A quantitative approach based on areas flooded by the sea and areas of marine and continental deposition. Am. J. Sci. 294, 802–860.

Sano, Y., 1996. Fluxes of mantle and subducted carbon along convergent plate. Geophys. Res. Lett. 23, 2749–2752.

Savin, S.M., Douglas, R.G., Stelli, F.G., 1975. Tertiary marine paleotemperatures. Geol. Soc. Am. Bull. 86, 1490–1510.

Savin, S.M., Abel, L., Barrera, E., Hodell, D., Kennnett, J.P., Murphy, M., Keller, G., Killinglley, J., Vincent, E., 1985. The evolution of Miocene surface and near-surface marine temperatures: Oxygen isotopic evidence. In: Kennett, J.P., Shackleton, N.J. (Eds.), The Miocene Ocean: Paleoceanography and Biogeography. Geol. Soc. Am. Mem. 63, pp. 49–82.

Shackleton, N.J., 1984. Oxygen isotope evidence for Cenozoic climate change. In: Brenchley, P. (Ed.), Fossils and Climate. Wiley, London, pp. 27–34.

Shackleton, N.J., Hall, M.A., 1984. Carbon isotope data from Leg 74 sediments. In: Moore, T.C. Jr., Rabinowitz, P.D., et al. (Eds.), Initial Reports of the DSDP 74. U.S. Government Printing Office, Washington, DC, pp. 613–719.

Shackleton, N.J., Kennett, J.P., 1975. Paleotemperature history of the Cenozoic and the initiation of Antarctic glaciation: Oxygen and carbon isotope analyses in DSDP Sites 277, 279 and 281. In: Kennett, J.P., Houtz, R.E., et al. (Eds.), Initial

Reports of the DSDP 29. U.S. Government Printing Office, Washington, DC, pp. 743–755.

Shackleton, N.J., 1987. The carbon isotope record of the Cenozoic: History of organic carbon burial and of oxygen in the ocean and atmosphere. In: Brooks, J., Fleet, A.J. (Eds.), Marine Petroleum Source Rocks. Geological Society of London Special Publication 26, pp. 423–434.

Shackleton, N.J., Hall, M.A., Bleil, U., 1985. Carbon Isotope Stratigraphy, Site 577. In: Harth, G.R., et al. (Eds.), Initial Reports of the Deep Sea Drilling Project 86. U.S. Government Printing Office, Washington, DC, pp. 503–511.

Shikazono, N., 2003. CO_2 flux due to hydrothermal venting from back-arc basin and its influence on global carbon cycle. Geology (submitted).

Shikazono, N., 1998. Hydrothermal activity and global CO_2 cycle in Cenozoic (in Japanese, with English abstract). J. Geogr. 107, 127–131.

Shikazono, N., 1999. Carbon dioxide flux due to hydrothermal venting from back-arc basin and island arc and its influence on the global carbon dioxide cycle. Abstract Ninth Annual V.M. Goldschmidt Conference, p. 272.

Tajika, E., 1998. Climate change during the last 150 million years: Reconstruction from a carbon cycle model. Earth Planet. Sci. Lett. 160, 696–707.

Tatsumi, Y., Otofuji, Y., Matsuda, T., Nohda, S., 1989. Mechanism of backarc opening in the Japan sea; role of asthenospheric injection. Tectonophysics 181, 299–306.

Tsunakawa, H., 1981. Ancient Stress Field in Japan Based on K–Ar Ages of Neogene Dikes and Boninite. Ph.D. Thesis, University of Tokyo, 134 pp.

Vidal, P., Cocherie, A., Le Fort, P., 1982. Geochemical investigations of the origin of the Manaslu leucogranite (Himalaya, Nepal). Geochim. Cosmochim. Acta 46, 2279–2292.

Vincent, E., Berger, W.H., 1985. Carbon dioxide and polar cooling in the Miocene: the Monterey hypothesis. In: Sundquist, E.T., Broecker, W.S. (Eds.), The Carbon Cycle and Atmospheric CO_2: Natural Variations Archean to Present. Geophysical Monograph 32, pp. 455–468.

Volk, T., 1987. Feedbacks between weathering and atmospheric CO_2 over the last 100 million years. Am. J. Sci. 287, 763–779.

Wolfe, J.A., 1978. A paleobotanical interpretation of Tertiary climates in the Northern Hemisphere. Am. Sci. 66, 694–703.

Woodruff, F., Savin, S.M., 1989. Miocene deepwater oceanography. Paleoceanography 4, 87–140.

Yamanoi, T., 1993. Paleo-vegetation in Japanese Islands in Neogene (in Japanese). Gekkan Chikyu 16, 180–185.

Zachos, J.C., Lohmann, K.C., Walker, J.C.G., Wise, S.W., 1993. Abrupt climate change and transient climates during the Paleogene amarine perspective. J. Geol. 101, 191–213.

Zachos, J.C., Pagani, M., Sloan, L., Thomas, E., Billups, K., 2001. Trends, rhythms, and aberrations in global climate 65 Ma to Present. Nature 292, 686–693.

Zhao, W.-L., Morgan, W.-J., 1985. Uplift of Tibetan Plateau. Tectonics 4, 359–369.